# Spin-orbit effects in the surface state of Fe(001) revealed by full surface Brillouin zone mapping

E. Młyńczak,<sup>1,\*</sup> A. Surendran,<sup>1</sup> S. Shaju,<sup>1</sup> K. Freindl,<sup>1</sup> J.

Korecki,<sup>1</sup> E. Madej,<sup>1</sup> D. Wilgocka-Ślezak,<sup>1</sup> M. Szczepanik,<sup>2</sup> T.

Sobol,<sup>2</sup> I. Aguilera,<sup>3</sup> G. Bihlmayer,<sup>4</sup> S. Blügel,<sup>4</sup> and N. Spiridis<sup>1</sup>

<sup>1</sup>Jerzy Haber Institute of Catalysis and Surface Chemistry,

Polish Academy of Sciences, Niezapominajek 8, 30-239 Krakow, Poland

<sup>2</sup>National Synchrotron Radiation Centre SOLARIS,

Jagiellonian University, Czerwone Maki 98, 30-392 Kraków, Poland

<sup>3</sup>Institute for Theoretical Physics, University of Amsterdam,

and European Theoretical Spectroscopy Facility (ETSF),

Science Park 904, 1098 XH Amsterdam, The Netherlands

<sup>4</sup>Peter Grünberg Institut PGI, Forschungszentrum Jülich and JARA-Fundamentals of Future Information Technologies, 52425 Jülich, Germany

(Dated: July 16, 2025)

## Abstract

The electronic structure of Fe has been experimentally studied using angle-resolved photoelectron spectroscopy (ARPES) since the early days of photoemission. Yet, the existence and nature of the Fe(001) surface state remain a subject of ongoing debate. Fe(001) is considered a prototypical transition metal system and moreover, one of the key players in the spintronics research. Here, we present the electronic structure of Fe(001) epitaxially grown on Au(001), mapped by high-resolution ARPES within the entire surface Brillouin zone, to demonstrate for the first time the exact location and extent of the Fe(001) surface state. The experimental results are supported by the relativistic slab calculations performed using density functional theory (DFT). The surface state observed for the pristine Fe(001) surface vanishes after overnight rest of the sample in ultrahigh vacuum as well as after intentional exposure to 5 Langmuir of oxygen which proves that it is not topologically protected. in contrast to recent discussions in the literature. Furthermore, the dispersion of the surface state is found to depend on the relative orientation of the magnetization, which is explained based on the DFT results as related to the Rashba effect. These new experimental and theoretical results contribute to the existing knowledge on the electronic properties of Fe(001) with relevance for the basic research as well as for spintronic effects, such as tunneling anisotropic magnetoresistance.

#### I. INTRODUCTION

The surface electronic states, which occur due to breaking of the translational symmetry along the surface normal, exist for example at the surfaces of noble metals: Au(111), Ag(111) and Cu(111), where they form well-defined sp-like parabolic states centered around the  $\overline{\Gamma}$  point [1].

The surfaces of transition metals are also known to host surface states formed by dangling d bonds [2, 3], but also sp-like states are observed as in the case of Ni(111) [4]. The surface states and surface resonances have been theoretically described and experimentally observed for Fe(110) surface [5–10], also in the form of Fermi arcs [11], related to the postulated topologically nontrivial nature of Fe [12, 13].

The surface states of Fe(001) are particularly important due to their technological relevance, as the interfacial resonance states in the Fe/MgO/Fe magnetic tunnel junction [14] are inherited from the surface states of clean Fe(001) [15, 16]. Moreover, the dependence

of the Fe(001) surface state on the magnetization direction due to spin-orbit coupling has been recognized as a source of the tunneling anisotropic magnetoresistence, which allows the spin-dependent tunneling in devices with single Fe(001) electrode [17]. Also, the electric-field induced change of the minority surface state of Fe(001) was found theoretically to be responsible for the electric-field modification of magnetic anisotropy in ultrathin Fe(001) films [18]. In addition, the spin-orbit effects in Fe thin films are also relevant for the closely related system of oxygen-passivated Fe(001)-p(1 × 1)O surface, which is nowadays routinely used in spin-detectors that rely on both exchange and spin-orbit spin-dependent electron scattering [19].

The surface states of Fe(001) have been studied experimentally even before their role in spintronics was revealed. Due to technical limitations, previous experimental works focused on the identification of the surface state only in the very center of the surface Brillouin zone [2, 20-22] or along the  $\overline{\Gamma} - \overline{X}$  line [16, 23]. Already in 1983, the surface electronic structure of Fe(001) has been investigated using synchrotron-based angle-resolved photoemission spectroscopy (ARPES) by Turner and Erskine [23] and the two surface states, lying within the projected band gap of the bulk electronic states, have been identified. By comparison to the early slab calculations, one of these states, lying directly below the Fermi level (also at the very  $\Gamma$  point) has been identified as the minority-spin state, while the other, located approximately at the binding energy of 2 eV, has been identified as its majority-spin counterpart. In the following years, the Fe(001) surface state in the center of the surface Brilluoin zone ( $\Gamma$ point) lying directly below the Fermi level has been claimed by Vescovo et al. to be of the majority-spin character [20]. On the other hand, Stroscio et. al. have shown using scanning tunneling spectroscopy the existence of the unoccupied surface state along the surface normal, which was interpreted as minority-spin by comparison with the slab calculations [2]. This interpretation was later verified experimentally by spin-polarized photoemission on the potassium covered Fe(001) [21] and by spin-polarized inverse photoemission [22]. In 2009, Plucinski et al. have shown spin- and angle-resolved spectra for Fe(001) films grown on W(001), along the entire  $\overline{\Gamma} - \overline{X}$  line and demonstrated the existence of the occupied minority surface state along most of the  $\overline{\Gamma} - \overline{X}$  distance, which however disappears at both  $\overline{\Gamma}$ and  $\overline{X}$  [16]. In recent years some of us have extensively studied the electronic structure of Fe(001) films grown on Au(001) [24–27] and found no signatures of the surface states in the experimental band structures measured both using lab-based high-resolution ARPES with  $E_{h\nu}=16.8~eV$  [24] as well as in the k-space microscopy studies performed using  $E_{h\nu}=70$  eV [25–27].

Here, we present experimental results that demonstrate the existence of the Fe(001) surface state for Fe films grown on Au(001), using the same recipe as for the samples discussed in [24–27], but prepared in another deposition system. We suspect that the presence of this surface state is extremely sensitive to the adsorption of the residual gases, which are inherently present in ultrahigh vaccum chambers. We demonstrate by ARPES and relativistic slab calculations the minority surface state of Fe(001) of a four petal-likeflower shape at the Fermi level, with the petals aligned with  $\overline{\Gamma} - \overline{X}$  and disappearing near  $\overline{\Gamma}$ , as theoretically predicted by Chantis et al. [15, 17, 28]. The photon energy dependence, significant energy broadening as well as lack of full symmetry with respect to the border of the surface Brillouin zone point to the surface resonant character of the observed surface state at least close to the  $\overline{X}$  points, which is in accord with the theoretical predictions of the weak mixing of this state with the bulk bands [17]. We show that the surface state surrounds in the immediate vicinity of the  $\overline{X}$  points exhibits strongly asymmetric dispersions that can be explained by the Rashba-type effect. Our findings support the importance of the spin-orbit coupling for the electronic structure of materials even as light as Fe.

#### II. EXPERIMENTAL AND THEORETICAL METHODS

The entire experiment was performed in the Phelix end-station at the SOLARIS National Synchrotron Radiation Centre in Kraków [29]. Fe films were grown in the Phelix preparation chamber. Au(001) crystal was cleaned by cycles of Ar sputtering and annealing at T=800K for 10 minutes until a c(28 × 48) surface reconstruction characteristic for a clean Au(001) crystal [30] was clearly visible in low energy electron diffraction (LEED) [Supplementary Fig. S1 (a)]. Fe films were deposited on such prepared Au(001) single crystal at low temperature (T=100K) using molecular beam epitaxy and gently annealed up to 800K. This preparation procedure was found previously to result in high quality Fe(001) films, with no Au present on the Fe surface [24]. In the currently reported experiments we have also used x-ray photoelectron spectroscopy (XPS) to verify cleanliness of the pristine Fe(001) surface [Supplementary Fig. S2]. Fe(001) grows on Au(001) following the epitaxial relationship: bcc Fe[100] [] fcc Au[110], which was verified using LEED [Supplementary Fig. S1 (b)].

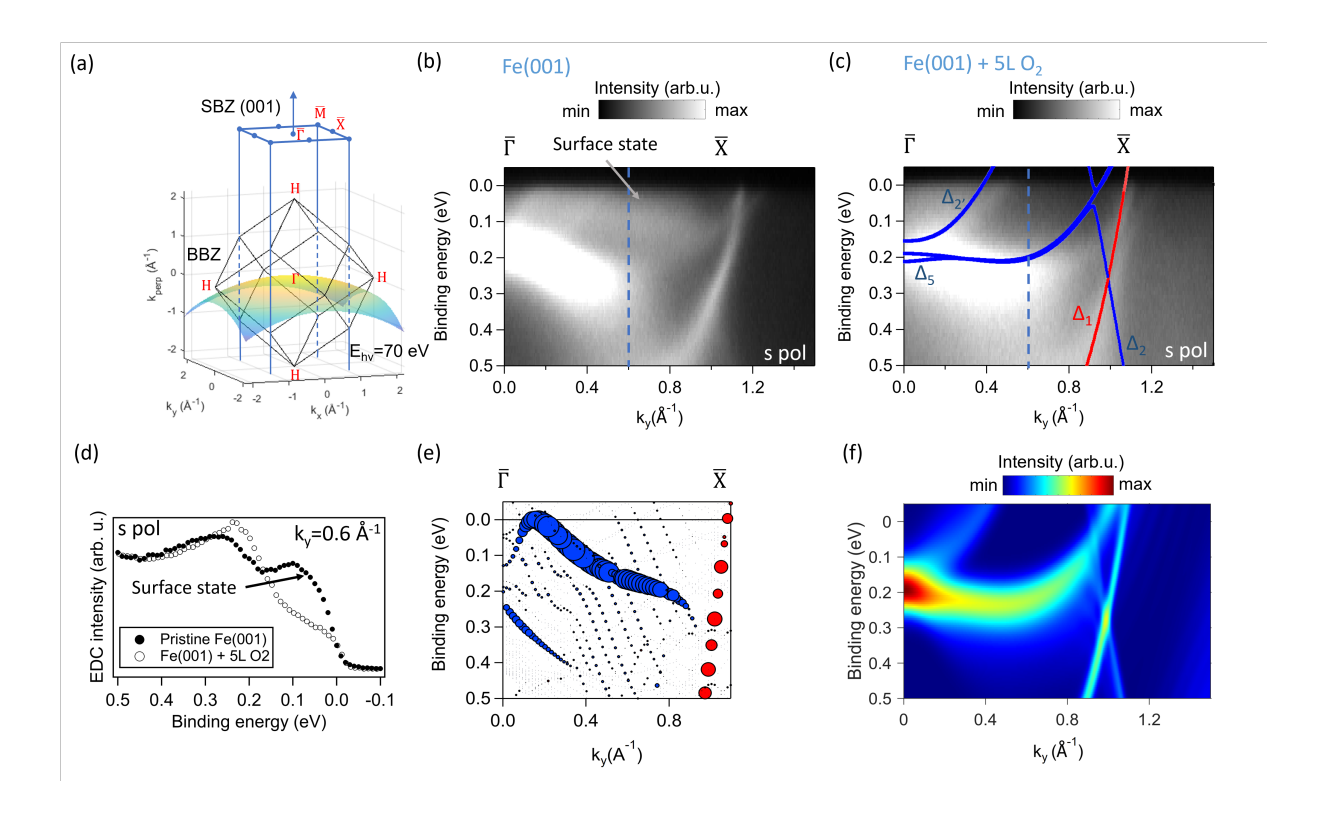


FIG. 1. (a) A sketch of the bulk Brillouin zone (BBZ) of bcc Fe and Fe(001) surface Brillouin zone (SBZ). The colored surface indicates the  $k_{\perp}^0$  wavevectors accessed by photoemission excited with  $E_{h\nu}=70$  eV photons, according to free electron final state model. (b) Angle-resolved photoemission spectrum measured along the  $\overline{\Gamma}$  -  $\overline{X}$  direction for a pristine Fe(001)/Au(001) surface using  $E_{h\nu}=70$  eV and s-polarized light. An arrow points to the identified surface state. (c) The same as (b) for the sample exposed to 5 L of oxygen. The surface state from (b) is not present. The blue/red lines indicate bulk minority/majority states as given by the results of the GGA calculation. The dashed blue lines in (b) and (c) mark position of energy distribution curves presented in (d). (d) Energy distribution curves (EDC) derived from spectra in (b) and (c) at  $k_y=0.6\text{\AA}^{-1}$  for a pristine Fe(001) surface (full symbols) and after exposure to 5L of oxygen (empty symbols). The identified surface state is marked by an arrow. (e) The result of the GGA slab calculation of the surface electronic structure of Fe(001). Blue/red markers correspond to the minority/majority states. Size of the marker is proportional to the localization of a particular state in the surface region. (f) Result of the photoemission simulation performed starting from the GGA bulk band structure that takes into account the  $k_{\perp}$  broadening.

The minute in-plane lattice mismatch between Fe(001) and Au(001) which equals to 0.6%, promotes high-quality epitaxial growth, which is proven by very sharp Fe(001) LEED spots with negligible background [Supplementary Fig. S1 (b)]. The major experimental studies, including oxygen adsorption experiment were done on films with a thickness of approximately 80 monolayers (ML). A thinner film (40 ML-thick) was grown for comparison and monitored after overnight rest in ultrahigh vacuum conditions. Both film thicknesses showed qualitatively the same picture of the Fe(001) surface state. The samples were remanently magnetized in situ using a permanent magnet, mounted on the PTS-type sample holder, directly after growth. A photograph of the used setup is included in Supplementary Fig. S1 (c). The magnetic field generated by the permanent magnet (approximately 140 mT) is much more than the coercivity of a thin Fe film grown on Au(001), being typically of the order of 1 mT [31]. The samples were magnetized along Fe[100] direction, which is an easy axis dictated by the magnetocrystalline anisotropy of Fe(001). The Curie temperature of the studied Fe films is well above the room temperature [32]. Photoemission experiments were performed at the Phelix beamline using angle-resolved electron energy analyzer from SPECS which operates with scanning lenses system that facilitate mapping of the electronic dispersions. In order to map the entire surface Brillouin zone of Fe(001) it was necessary to employ in addition change of the polar and azimuthal angles. Specifically, to access X points that differ due to symmetry breaking by the in-plane magnetization, we changed the azimuthal angle. For the measurements around the  $\overline{\Gamma}$  ( $\overline{X}$ ) point, the synchrotron light reaches the sample at the angle of 54.7° (39.7°) with respect to sample normal. A six-axis manipulator was cooled with liquid helium during ARPES measurements. Most of the measurements were performed using photon energy of  $h\nu = 70$  eV and s- or p- polarized light. The oxygen adsorption experiment was performed using high purity oxygen gas dosed by a leak valve in the preparation chamber to the total dose of 5 Langmuir (L). Such a dose is expected to lead to the oxygen coverage close to a monolayer and is still well below the exposure that would result in a surface oxide layer. The chemical state of Fe after oxygen adsorption was monitored using XPS and the amount of the adsorbed oxygen was estimated to be equal to a monolayer [Supplementary Fig. S2]. In addition, constant energy maps were acquired using a range of photon energies, between 55 eV and 125 eV and p-polarized light.

First-principles calculations were carried out within the all-electron full-potential lin-

earized augmented-plane-wave (FLAPW) formalism with the FLEUR [33] code. For the bulk GGA calculations, we used an angular momentum cutoff of  $l_{\text{max}} = 8$  in the atomic spheres and a plane-wave cutoff of 5.0 bohr<sup>-1</sup> in the interstitial region. We used an experimental bcc Fe lattice parameter of 2.87 Å. The 3s and 3p orbitals were treated as semicore by the use of local orbitals. We used a  $10 \times 10 \times 10$  k-point sampling of the Brillouin zone.

To study Fe(001) surface states, the GGA slab calculation was performed using a 27 layer film with an angular momentum cutoff of  $l_{\text{max}} = 8$ , a plane-wave cutoff of 3.8 bohr<sup>-1</sup> and  $12 \times 12 \times 1$  k points. For the in-plane lattice constant, a theoretical GGA value of bulk Fe was used, i.e. 2.83 Å, which allowed for correct relaxation of the thin film interlayer spacings that was found to be equal to  $d_{12} = -0.65\%$ ,  $d_{23} = +3.95\%$ ,  $d_{34} = 1.33\%$ , and  $d_{45} = 0.05\%$ . Determination of the localization of electronic states within the surface region was performed according to the contribution within the atomic spheres in the upper two layers.

To simulate the photoemission spectrum based on the bulk initial band structure, we use the same scheme as described in detail in Ref. [26]. In short, we take into account the experimental energy broadening ( $\Delta E=20 \text{ meV}$ ) as well as the broadening in the perpendicular wavevector ( $\Delta k_{\perp}=0.33 \text{ Å}^{-1}$ ) related to the escape depth of the photoexcited electron via the Heisenberg principle. The value of  $\Delta k_{\perp}$  was found by adjusting the simulation result to the experimental data.

To obtain the photoemission intensity, we integrate the initial state spectral function in  $k_{\perp}$ : [34, 35]

$$I(E^{f}, E^{i}) \propto \int_{-\infty}^{\infty} dk_{\perp} |T^{f}|^{2} |M_{fi}(k_{\perp})|^{2} \cdot \frac{\Delta k_{\perp}}{(k_{\perp} - k_{\perp}^{0})^{2} + (\Delta k_{\perp}/2)^{2}} \cdot \frac{\Delta E}{(E^{i} - E^{i}(k_{\perp}^{0}))^{2} + (\Delta E/2)^{2}}$$
(1)

 $E^i(k_{\perp}^0)$  is an input to the simulation given by the result of the GGA *ab initio* calculation of the bulk electronic structure. In our simulations, we assume the final state surface transmission  $(T^f)$  and photoexcitation matrix elements  $(M_{fi})$  to be equal to unity. The value of  $k_{\perp}^0$  is determined using the free electron final state model with the inner potential  $V_0$ =11 eV, where  $E_{kin}$  is the kinetic energy of the photoexcited electrons, while  $\Theta$  is the emission

angle:

$$k_{\perp}^{0} = \sqrt{(2m/\hbar^{2})(E_{kin}cos^{2}\theta + V_{0})}$$
 (2)

## III. EXPERIMENTAL AND THEORETICAL RESULTS

## A. Electronic band structure along the $\overline{\Gamma}$ - $\overline{X}$ direction

To facilitate orientation in the reciprocal space, a sketch of the bulk Brillouin zone of bcc Fe and a surface Brillouin zone of Fe(001) is shown in Fig. 1 (a). The Fe  $\langle 100 \rangle$  directions correspond to the  $\Gamma$ -H ( $\Delta$ ) directions in the reciprocal space.  $\Gamma$ -H ( $\Delta$ ) directions project to the (001) surface as a  $\overline{\Gamma}$  -  $\overline{X}$  direction within the surface Brillouin zone. The colored surface represents values of the  $k_{\perp}^0$  wavevectors accessed in our photoemission experiment. The electronic band structure measured for a pristine Fe(001)/Au(001) surface using  $E_{h\nu}=70~{\rm eV}$ and s-polarized light along the  $\overline{\Gamma}$  -  $\overline{X}$  line is presented in Fig. 1 (b). The results obtained for ppolarized light are presented in the Supplementary Information, Fig. S3. The photoemission spectrum measured after oxygen adsorption is presented in Fig. 1 (c). An experiment of oxygen adsorption is a well-established procedure to distinguish the surface states from the bulk states [5, 16, 20, 22, 23]. Both spectra, before and after oxygen adsorption, can be compared to the bare GGA bulk bands along the  $\Gamma$ -H ( $\Delta$ ) line, which are shown as an overlay in Fig. 1 (c), where the blue/red color shows the predominantly minority/majority spin character of the bulk bands. The experimentally observed broadening of the electronic states in the Fermi level region is caused mostly by the spread of the allowed  $k_{\perp}$  vectors that results from the uncertainty principle [26]. The photoemission simulation performed within the scheme described in Ref. [26] that involves the  $k_{\perp}$  broadening, based on the bulk bcc Fe band structure as given by the GGA is presented in Fig. 1 (f). It is important to note that the spectrum of clean Fe(001) [Fig. 1 (b)] shows high spectral weight between the minority  $\Delta_5$  band and the Fermi level, where there are no bulk states expected close to the Fermi level, for  $k_y$  wavevectors between approximately 0.5 and 0.8  $\text{Å}^{-1}$  and for the projection of  $k_{\perp}$  close to the bulk  $\Gamma$  point, even when the projection of  $k_{\perp}$  is taken into account [Fig. 1 (f). On the other hand, the photoemission spectrum measured after oxygen adsorption [Fig. 1 (c)] shows much smaller spectral intensity in the same region, which points to the

surface character of the state observed for a pristine surface. In the same time, such strong damping of the surface state by oxygen adsorption indicates that the state is topologically trivial.

In addition, we present results of the GGA-based slab calculations of the surface electronic structure of Fe(001) along the  $\overline{\Gamma}$  -  $\overline{X}$  line [Fig. 1 (e)]. Here, the size of the symbol corresponds to the localization of the state in the surface region, while the blue/red colors mark predominantly minority/majority states. Clearly, the minority surface state is expected by theory along this k-space direction, right below the Fermi level, dispersing slightly towards deeper binding energies for larger k values. It consists of a combination of  $d_{xz}$  and  $d_{yz}$  orbitals and is well-recognized in the literature thanks to the earlier theoretical studies [2, 16, 36]. The spectrum of a clean Fe(001) surface [Fig. 1 (b)] shows also an intense parabolic-like state that passes the Fermi level close to the X point. This parabolic-like state survives the oxygen adsorption, therefore we interpret it as a bulk majority  $\Delta_1$  state, even though its energetic position and dispersion is similar to the theoretically predicted majority surface state [Fig. 1 (e)]. In addition, energy distribution curves (EDC) derived from the measured 2D spectra for  $k_y = 0.6\text{\AA}^{-1}$ , are presented in Fig. 1 (d). Clearly, the surface state observed for the pristine surface (full symbols) is quenched after oxygen adsorption (open symbols). The considerable energy spread of the observed surface state, which is close to 100 meV, can be partially attributed to the scattering-related lifetime effects, which are significant in Fe, even in the minority-spin channel [37]. On the other hand, the theoretical considerations of Chantis et al. [17] on the nature of the four-petal Fe(001) minority surface state include broadenings of this state due to coupling with both minority and majority spin bulk bands. Spin-flip scattering that govern tunneling magnetoresistance is theoretically expected to depend strongly on this intrinsic width of the resonant surface states [38].

## B. Fermi surface in the vicinity of the $\overline{\Gamma}$ point

In this section we will discuss the electronic band structure in the center of the surface Brillouin zone of a pristine Fe(001) surface [Fig. 2 (a)], in comparison to the oxygen-adsorbed Fe(001) [Fig. 2 (b)]. The result of the GGA-based slab calculation is presented in Fig. 2 (c), while the result of the bulk GGA calculation is shown in Fig. 2 (d) [the method used here is the same as in Fig. 1 (e)]. The electronic state visible in the vicinity of the  $\overline{\Gamma}$  point for

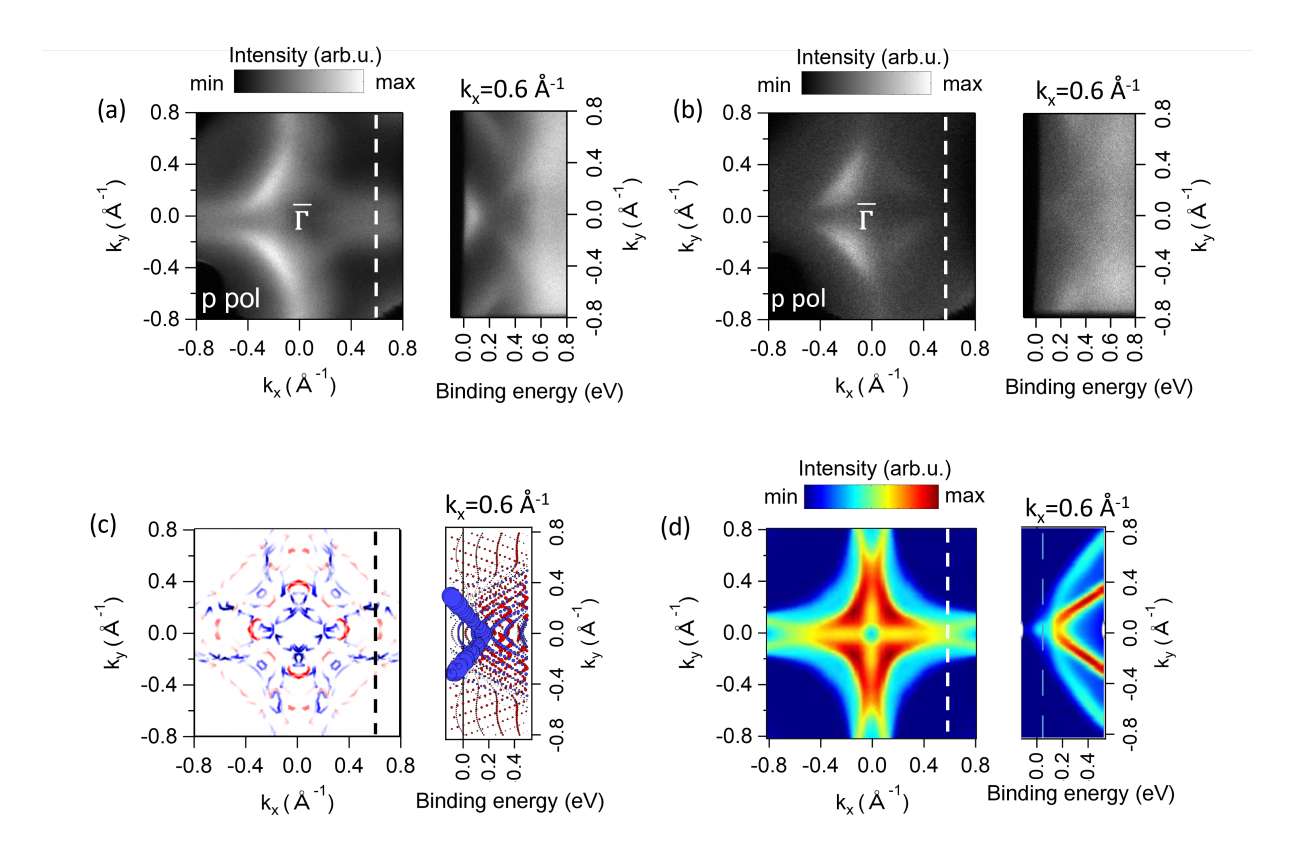


FIG. 2. Constant energy cuts near the Fermi level together with dispersions along the  $k_x = 0.6\text{Å}^{-1}$  line. (a) The electronic band structure measured in the vicinity of the  $\overline{\Gamma}$  point for a pristine Fe(001) surface. (b) The same as (a) after adsorption of 5 L of oxygen. In Figures (a) and (b) synchrotron light comes from the right. (c) The result of the surface electronic structure calculation with blue/red color that indicate minority/majority states and the size of the symbol represents localisation of the state in the surface layer. (d) Result of the photoemission simulation based on the bulk GGA calculation that takes into account  $k_{\perp}$  broadening.

clean Fe(001) surface within the  $(k_x, k_y)$  plane slightly deviates from four-fold symmetric, with some intensity difference visible between the negative and positive  $k_x$  values related to the symmetry breaking by the light incidence direction (the synchrotron light is coming from the right of the image). The intensity at the very  $\overline{\Gamma}$  point is much smaller than in the surrounding region. Such a picture could be in principle consistent with the bulk electronic structure predicted by the GGA *ab initio* calculations [Fig. 2 (d)], as well as with the surface state predicted by the slab calculation [Fig. 2 (c)]. The feature that helps to distinguish the two is the dispersion of the state observed close to the  $k_x = 0.6\text{\AA}^{-1}$  line. The experiment

for a pristine Fe(001) surface shows the electron-like dispersion of this state, exactly as the one predicted by the slab calculation for the surface state [Fig. 2 (c)], in contrast to the hole-like (dispersing 'downwards') bulk state [Fig. 2 (d)]. The spectra observed after oxygen adsorption [Fig. 2 (b)] support this picture. Apparently, the four-fold symmetric petal-like state that was spreading from the vicinity of the  $\overline{\Gamma}$  point towards the  $\overline{X}$  point and was clearly visible at  $k_x = 0.6\text{\AA}^{-1}$  got suppressed by the oxygen adsorption. The state that survived the adsorption is the theoretically predicted bulk state.

The results of the complementary measurements performed using p-polarized light, as well as additional cuts along  $k_x = -0.6\text{Å}^{-1}$  lines are presented in the Supplementary Materials, Fig. S4.

# C. Fermi surface in the vicinity of the $\overline{X}$ point. Rashba effect.

Figure 3 presents the experimental data collected in the vicinity of two  $\overline{X}$  points using p-polarized light for a pristine and oxygen-covered Fe(001) surface. The two  $\overline{X}$  points are distinguished due to their positions with respect to the magnetization direction. The  $\overline{X}_1$  ( $\overline{X}_2$ ) point lies on the  $\overline{\Gamma}$ - $\overline{X}$  line perpendicular (parallel) to the magnetization direction as shown on the sketch of the surface Brillouin zone in Fig. 3 (a). The symmetry of the thin film under investigation is lowered with respect to the symmetry of the bulk crystal by the presence of the sample surface which breaks the translational symmetry and also by the magnetization vector which lies in the sample plane. As a result, the only symmetry operation that is left is a single mirror plane which is perpendicular both to the sample surface and to the in-plane magnetization (the  $\overline{\Gamma}$ - $\overline{X}_1$  line lies within that mirror plane). Consequently, the electronic band structure that we observe around the  $\overline{X}_1$  point is symmetric with respect to the  $\overline{\Gamma}$ - $\overline{X}_1$  line, both for the pristine surface, which shows the surface state [Fig. 3 (a)] and for the oxygen-covered surface [Fig. 3 (b)]. We observe also in this region of the surface Brillouin zone that the surface state disappears after oxygen adsorption Fig. 3 (a) and (b). In addition, after oxygen adsorption we observe apparent sharpening of the features at the Fermi surface that we mark with  $\alpha$ - and  $\alpha$ + labels, in analogy to the terminology used in [24]. According to [39], this effect can be attributed to the narrowing of the d-bands as a result of enhanced electron-electron correlations caused by the oxygen adsorption. Additional momentum-distributions curves derived from the discussed constant

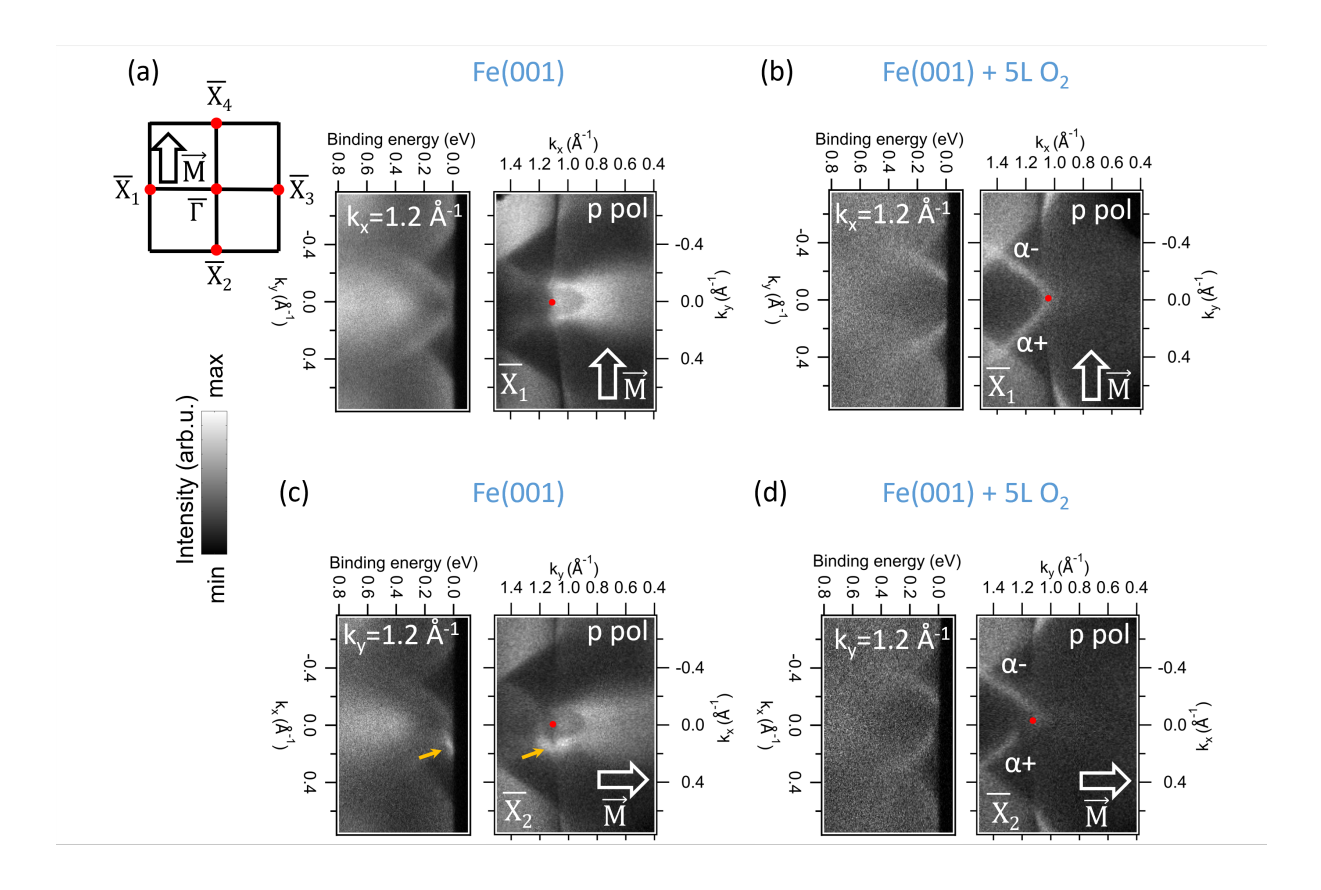


FIG. 3. The experimental electronic band structure measured in the vicinity of the two  $\overline{X}$  points using p-polarized light. (a) and (c) for pristine Fe (001) surface and (b) and (d) for the oxygen-covered Fe(001). The  $\overline{X}$  points differ due to different positions with respect to the magnetization direction as shown in the inset of (a). The  $\overline{X}_1$  ( $\overline{X}_2$ ) point lies on the  $\overline{\Gamma}$ - $\overline{X}$  line perpendicular (parallel) to the magnetization direction. The orange arrows in (c) point to the surface state located within the asymmetric spin-orbit gap. In Figures (a) and (b) synchrotron light comes from the right, and in figures (c) and (d) from the bottom of the images.

energy maps are presented in the Supplementary Information, Fig. S5.

Breaking of the symmetry by the presence of the sample surface and in-plane remanent magnetization is manifested by the asymmetrical electronic band structure. More specifically, for the oxygen-covered surface [Fig. 3 (d)] we observe that  $\alpha$ - and  $\alpha$ + features are not the same (as it is in the case of the  $\overline{X}_1$  point). The  $\alpha$ + feature is clearly shifted from the  $\overline{X}_2$  point (marked by a red dot), which is a manifestation of the opening of the spin-orbit gap. This effect was observed previously by some of us in the same sample system for 100-ML Fe films [24]. Opening of the spin-orbit gap near the  $\overline{X}$  point is predicted by the bulk calcula-

tion of the electronic band structure, however the bulk consideration does not capture the lowered symmetry observed for a thin film [24]. Interestingly, in the experiment that we are reporting here, we had access also to the pristine Fe(001) surface, and we can analyze the position/location of a surface state with respect to the bulk states for such an asymmetric case. Figure 3 (c) shows clearly that the intense state at the Fermi level is visible only for the positive  $k_x$  values [marked by yellow arrows in Fig. 3(c)], and is located exactly within the asymmetric spin-orbit gap of the bulk states [Fig. 3(d)].

Now we will compare the experimentally observed asymmetric surface state with the prediction of the *ab initio* calculation of the surface electronic structure. This is presented in Fig. 4. Here, again the size of the symbol corresponds to the localization of the state in the surface layer, and blue color indicates the minority spin character. The cut through the band structure is performed at  $k_x(y) = 1.2\text{Å}^{-1}$  along the wavevector perpendicular [Fig. 4 (a)] and parallel [Fig. 4 (b)] to the magnetization direction. Clearly, the minority surface state is asymmetric for the former case, and symmetric for the latter. The two branches of the surface state are shifted on the energy scale for the asymmetric case and the separation between them reaches  $\Delta E = 64$  meV. In the GGA result, the surface state is located above the theoretical Fermi level for these  $E_{x(y)}$  cuts, while in the experiment its lower branch is occupied [Fig. 4 (c)].

The asymmetry with respect to **k** observed both in the experiment and in the calculation can be explained as a Rashba-type interaction [40]. Rashba effect occurs upon inversion symmetry breaking e.g. at the surface. The surface potential gradient affects the Bloch wavefunctions of the conduction electrons such that they experience a momentum-dependent effective magnetic field leading to spin-momentum locking. In the case where spin-orbit coupling coexists with exchange interaction, a single-particle energy can be defined by the formula introduced in Ref. [41]. If the magnetization is aligned antiparallel to the y-axis, this reads:

$$\epsilon_{\mathbf{k}\sigma} = \frac{\hbar^2}{2m} [(k_x + \sigma k_0)^2 + k_y^2] - E_R - \sigma [(J_0 S)^2 + (\alpha_R k_y)^2]^{1/2}, \tag{3}$$

where  $\sigma$  is the spin quantum number  $\sigma = \pm 1$ ,  $\alpha_R$  is the Rashba parameter,  $k_0$  is the momentum shift  $(k_0 \propto \alpha_R)$ ,  $E_R$  is the energy shift  $(E_R \propto \alpha_R^2)$  and  $J_0S$  represents exchange splitting. According to Eq.(3), the band shift is expected for the in-plane wavevectors perpendicular to the magnetization direction, which is exactly what is observed in the ex-

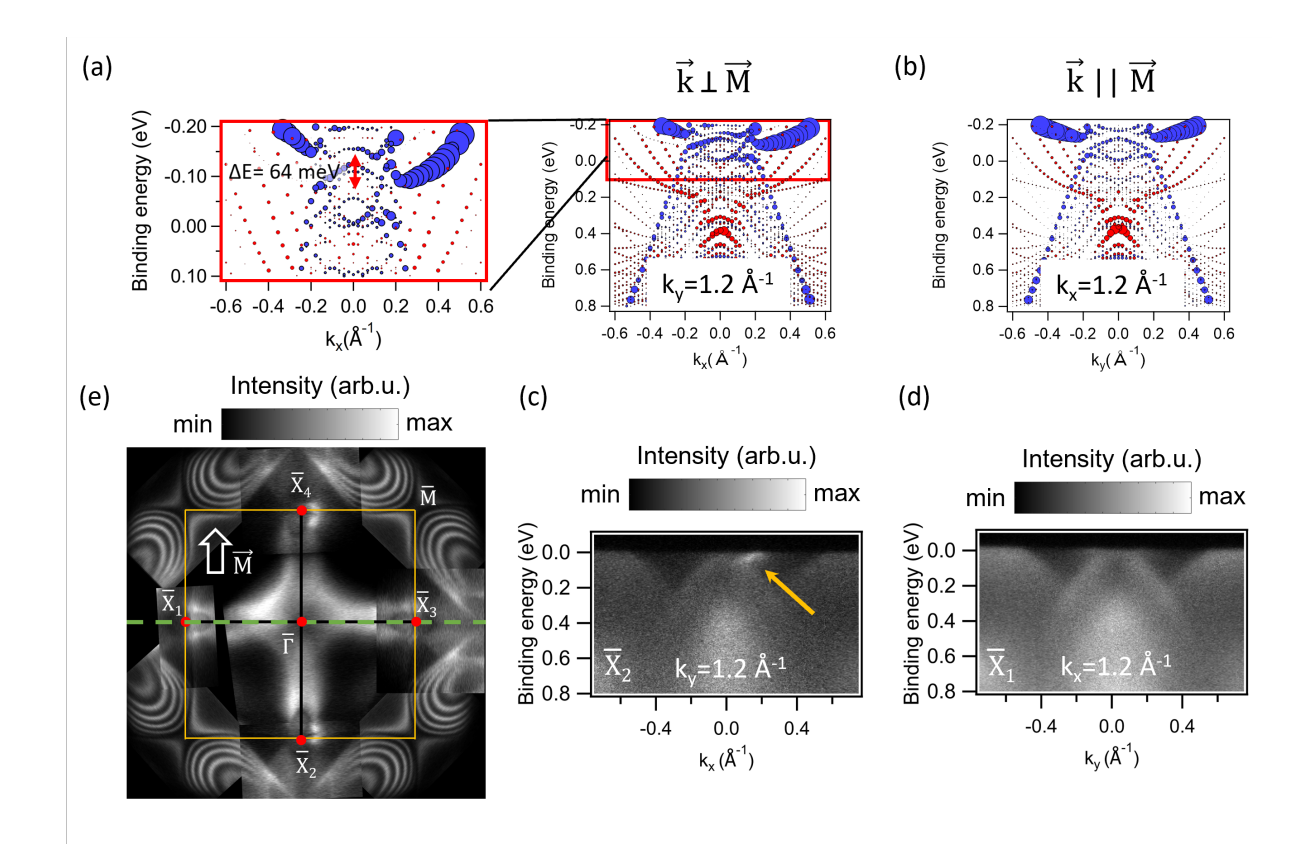


FIG. 4. The theoretical electronic band structure in the vicinity of two  $\overline{X}$  points obtained by the GGA slab calculation along the wavevector (a) perpendicular and (b) parallel to the magnetization direction. The size of the symbol corresponds to the localization of the state within the surface layer. In (a) a zoomed-in region directly above the theoretical Fermi level is shown within the red box. (c) and (d) are the same as in Fig. 3 (a) and (c), reproduced here for an easier comparison with the theoretical result. (e) Illustration of the studied surface state within the surface Brillouin zone for the 40ML-Fe(001) film constructed from individual measurements taken with 70 eV photons and p-polarized light. The green dashed line marks the mirror plane valid when the light incidence direction (light comes from the bottom in central part of the illustration) is neglected.

periment [Fig.3 (c)]. Chantis et al. have theoretically predicted such Rashba effect for the studied here four-petal minority surface state of Fe(001), however in the other part of the surface Brillouin zone, namely closer to the  $\overline{\Gamma}$  point [17].

For nonmagnetic materials, where the Rashba effect is most commonly observed, it leads to the splitting of a spin-degenerate electronic band into two spin-polarized branches. The size of the Rashba effect  $(\alpha_R)$  depends on the strength of the electric field in the surface

region and on the size of the intra-atomic spin-orbit coupling. A typical example of the Rashba-effect is spin-splitting of a heavy metal Au(111) surface state. In Ref. [42], the influence of the intra-atomic spin-orbit coupling on the Rashba splitting has been analyzed by comparison of the interface states in  $p(1 \times 1)O/Lu(0001)$  (Z=71) and  $p(1 \times 1)O/Y(0001)$  (Z=39). The Rashba splitting has been observed in the former case and absent in the latter. The observation of the Rashba effect has also been reported for the magnetically-ordered materials, where the spin direction is governed by the exchange interaction [42–44]. Examples of magnetic systems where the Rashba effect was observed include: Gd(0001) and  $p(1 \times 1)O/Gd(0001)$  [43], Tb(0001) [42] and quantum wells of Co/W(110) [44]. On the other hand, the effect was found to be not-observable in Co/Mo(110), which was attributed to the weaker spin-orbit coupling of Mo with respect to W [44]. In the earlier work of some of us [24], the asymmetric spin-orbit gap of the bulk states measured for the Fe(001)/Au(001) was also interpreted as a Rashba-type effect. Here, we have shown for the first time experimentally such Rashba-type asymmetry for the surface states of an element as light as Fe, proving the relevance of spin-orbit coupling in this material.

We have performed ARPES experiments on a couple of pristine Fe(001)/Au(001) films, each time obtaining similar results. Particularly interesting are photoemission spectra recorded for a thinner film, of approximately 40 ML, as they reveal clear quantum well states formed by the bulk bands in the vicinity of the M point. The results obtained for that sample are presented in Fig. 4 (e) and in Fig. 5. In Fig. 4 (e) we present an illustration created by combining multiple measurements taken in different regions of the SBZ with 70 eV photons and p-polarized light. The part of the surface Brillouin zone in the vicinity of the  $\overline{\mathrm{M}}$  point was measured for one of the  $\overline{\mathrm{M}}$  points and symmetrized. The electronic states close to each of the  $\overline{X}$  points were measured separately by rotating the sample along normal. This illustration nicely captures the four petal-like shape of the Fe(001) surface state and asymmetry near the  $\overline{X}_2$  and  $\overline{X}_4$  points. The green dashed line in the figure marks the mirror plane perpendicular to the magnetization direction, which is valid when we neglect the light incidence direction (the light is coming from the bottom in the central part of the illustration). In Figure 5 we are presenting constant energy cuts near  $\overline{X}_1$  and  $\overline{X}_4$  points together with selected E(k) cuts, taken in the range  $k_{x(y)} = 0.95 - 1.2 \text{Å}^{-1}$  for a 40-ML Fe film. Figures 5 (a) and (b) contain results for a pristine Fe(001) surface. Clearly, the surface state (marked with yellow arrows), appears symmetric [Fig. 5 (a)] or asymmetric [Fig. 5

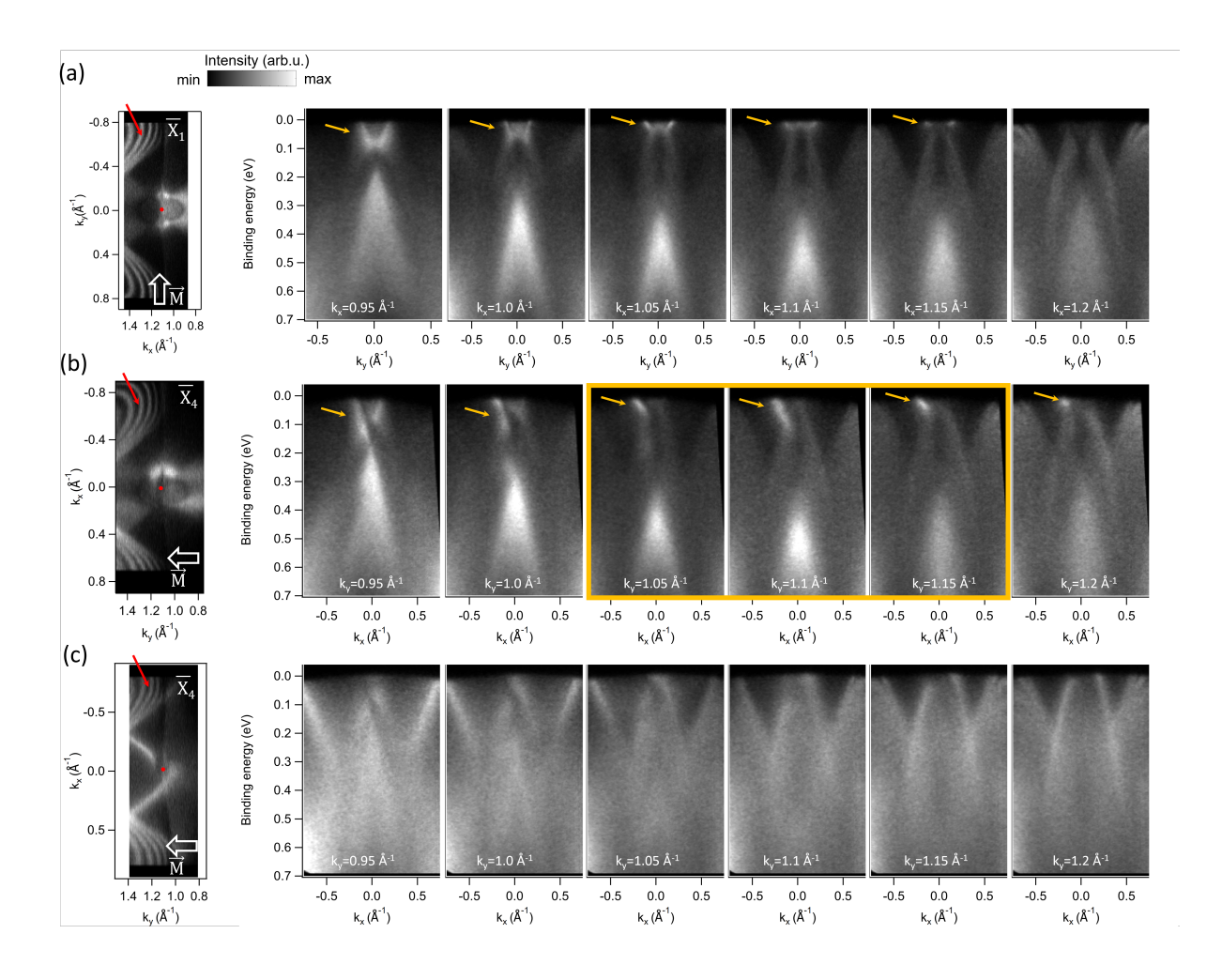


FIG. 5. (a) Constant energy map close to the  $\overline{X}_1$  point (left) together with a set of spectra taken for different values of  $k_y$  around the  $\overline{X}_1$  point, measured with  $E_{h\nu} = 70eV$  and p-polarized photons for a Fe film of 40ML. (b) The same as (a) but for the  $\overline{X}_4$  point. (c) The same as (b) but for the sample that was left in UHV overnight. In Figure (a) synchrotron light comes from the right and in Figures (b) and (c) from the top, when looking at the constant energy maps. The red arrows point to the quantum well states derived from the bulk bands while the yellow arrows point to the identified surface state. The yellow box frames the spectra that are symmetric with respect to the surface Brillouin zone border, indicating negligible mixing with the bulk states.

(b)] depending on the magnetization direction. The Fe(001) surface state is sensitive to the adsorption of the residual gases of the ultrahigh vacuum (UHV) chamber, as it disappears after overnight rest of the sample in the UHV conditions [Fig. 5 (c)].

In Figure 5 one can observe that  $E(k_x)$  cuts are not symmetric with respect to the surface Brillouin zone (SBZ) border  $(k_{x(y)}=1.1 \text{ Å}^{-1})$ , which would be expected for pure

surface states. The clear symmetrical behavior is observed only for the short range of  $k_y$ values directly near the  $\overline{X}_4$  point [Fig. 5 (c),  $k_y=1.05$ , 1.1, 1.15 Å<sup>-1</sup>, spectra surrounded by the yellow box. We can compare this experimental result to  $E(k_x)$  cuts near the SBZ border, as calculated by DFT (GGA). Such results are presented in Fig. 6. We see, that the previously identified asymmetric minority surface state (blue) which lies directly above the GGA Fermi level extends towards the occupied part of the band structure exactly at the border of the Brillouin zone  $(k_y=1.1 \text{ Å}^{-1})$ . Also, in the close vicinity of the SBZ border, this state has no or very little overlap with the quantum well states formed by the majority bulk states (band structures surrounded by the orange box). On the other hand, moving away from the SBZ border, we observe a clear overlap between the minority surface state and the majority bulk bands, which strongly suggests that this state turns into a surface resonance with the change in  $k_y$ , in accord with the previous theoretical predictions [38]. Moreover, we have performed photon energy dependent measurements in the vicinity of the X point, using a range of photon energies between 55 eV and 125 eV, which are presented in the Supplementary Information, Fig. S5. We see that the observed states, including those located along the  $\overline{\Gamma}$ - $\overline{X}$  line up to at least  $k_x$ =0.6 Å<sup>-1</sup> are visible only within a short range of photon energies (65 eV - 80 eV) indicating bulk-like character of surface resonances. We also note, that the clearly asymmetric surface state at the X point is observed only in even shorter range of photon energies (for 65 eV and 70 eV), which is related with its location within the asymmetric spin-orbit gap formed by the bulk bands at the  $\overline{X_2}$  and  $\overline{X_4}$  points.

As the last remark, we want to mention that in the analyzed set of the experimental data, which was limited in binding energy to approximately 1 eV below the Fermi level, we have not observed signatures of electronic quasiparticles such as those reported e.g for the surface state of Fe(110) due to electron-magnon coupling by J. Schäefer et al. [8, 9].

To picture the studied surface state within the surface Brillouin zone (SBZ), we have created an image combined from multiple measurements taken in different regions of the SBZ with 70 eV photons and p-polarized light for 40ML-thick Fe(001) film [Fig. 5 (e)]. The quantum well states in the vicinity of the  $\overline{\rm M}$  point were measured for one of the  $\overline{\rm M}$  points and symmetrized. The electronic states close to each of the  $\overline{\rm X}$  points were measured separately by rotating the sample along normal. This illustration nicely captures the four petal-like shape of the Fe(001) surface state and asymmetry near the  $\overline{\rm X}_2$  and  $\overline{\rm X}_4$  points. The green dashed line in the figure marks the mirror plane perpendicular to the magnetization

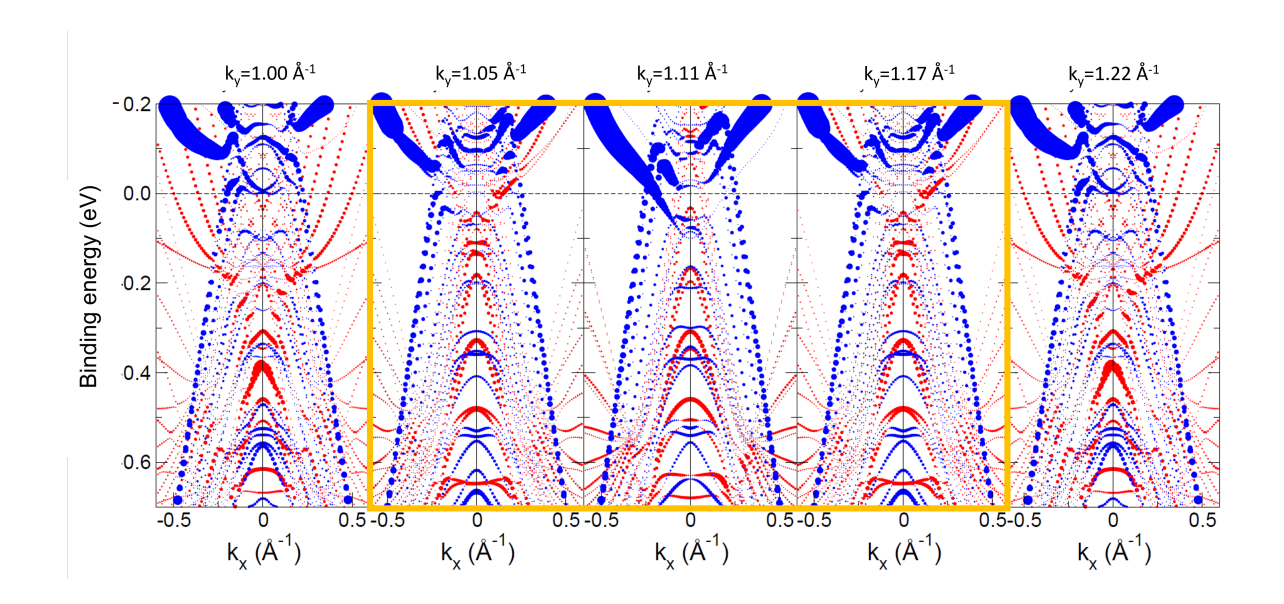


FIG. 6. The result of the surface electronic structure calculation with blue/red color that indicate minority/majority states and the size of the symbol represents localisation of the state in the surface layer.  $E(k_x)$  cuts for different  $k_y$  values in the vicinity of the surface Brillouin zone (SBZ) border  $(k_y=1.1 \text{ Å}^{-1})$ . The spectra outside from the first surface Brillouin zone are symmetrized with respect to the SBZ border.

direction, which is valid when we neglect the light incidence direction (the light is coming from the bottom in the central part of the illustration).

Having identified the intensities extending from the  $\overline{X}$  point towards the center of the surface Brillouin zone as a surface state, we have also performed mapping of the constant energy cuts near the Fermi level using a range of photon energies between 55 eV and 125 eV. The results of these measurements can be found in the Supplementary Information, Fig. S5. We have determined that the discussed surface state is visible at the scans performed using the photon energies between 65 eV and 80 eV, for higher (and lower) photon energies the cross section for photoemission is apparently too low to enable experimental observations of this state. Similar strong photon energy-dependent cross-section of a surface state was observed before e.g. for the surface state of Al(001) [45].

As the last point, we will shortly discuss the possible topologically-nontrivial character of the observed surface state. According to the calculations of Gosalbez-Martinez et al multiple Weyl nodes exist in the band structure of bcc Fe, including two topologically non-trivial ones located roughly midway between bulk  $\Gamma$  and H points, in the k-space region that is projected

onto the (001) surface very close to the  $\overline{X}$  point. The surface state observed by us to be located within the asymmetric spin-orbit gap of the bulk states close to the  $\overline{X}$  point has a characteristic line (arc) shape at the Fermi surface [Fig. 3 (c)], rather than a closed contour.

These clues suggest that the observed state could be a topologically non-trivial Fermi are related to the theoretically predicted Weyl nodes. On the other hand, the observed surface state is not robust against oxygen adsorption, which is expected if it was topologically-protected [46]. Therefore, we can conclude that the observed Fe(001) surface state is topologically trivial.

## IV. SUMMARY AND CONCLUSIONS

In this work, we have studied the electronic band structure of thin film Fe(001) epitaxially grown on Au(001). We have shown experimentally the extent of the occupied part of the Fe(001) minority surface state in energy and momentum. Experimental observation of the Fe(001) surface state was possible thanks to the superb surface cleanliness and careful tuning of the photon energy used in ARPES. The Fe(001) surface state extends below the Fermi level along the  $\overline{\Gamma} - \overline{X}$  lines, vanishing near  $\overline{\Gamma}$  and surrounding the  $\overline{X}$  points. The experimental data compare very well with the predictions of the surface electronic structure based on density functional theory (GGA). We have demonstrated that the surface state vanishes after overnight stay of the sample in UHV, as well as after intentional exposure of a fresh surface to 5 Langmuir of O<sub>2</sub>, therefore we conclude that it has a topologically-trivial nature. We have also shown that the studied surface state has a character of a surface resonance, at least in the k-space regions close to the  $\overline{X}$  points. In the immediate vicinity of the  $\overline{X}$  point, the surface state is asymmetric with respect to the  $\overline{\Gamma} - \overline{X}$  direction along which the sample is remanently magnetized, filling the asymmetric spin-orbit gap of the bulk bands. This asymmetry is captured by the results of the GGA slab calculations and can be interpreted as a Rashba-type effect.

#### ACKNOWLEDGEMENTS

This work was funded by the National Science Centre, Poland (NCN), grant number 2022/46/E/ST3/00184. This publication was partially developed under the provision of the

Polish Ministry and Higher Education project "Support for research and development with the use of research infra-structure of the National Synchrotron Radiation Centre SOLARIS" under contract no 1/SOL/2021/2. We gratefully acknowledge the computing time granted through JARA-HPC on the supercomputer JURECA at Forschungszentrum Jülich.

- \* ewa.mlynczak@ikifp.edu.pl
- [1] R. Paniago, R. Matzdorf, G. Meister, and A. Goldmann, Temperature dependence of shockley-type surface energy bands on Cu(111), Ag(111) and Au(111), Surface Science **336**, 113 (1995).
- [2] J. A. Stroscio, D. T. Pierce, A. Davies, R. J. Celotta, and M. Weinert, Tunneling spectroscopy of bcc (001) surface states, Phys. Rev. Lett. 75, 2960 (1995).
- [3] S. N. Okuno, T. Kishi, and K. Tanaka, Spin-polarized tunneling spectroscopy of Co(0001) surface states, Phys. Rev. Lett. 88, 066803 (2002).
- [4] M. Donath, F. Passek, and V. Dose, Surface state contribution to the magnetic moment of Ni(111), Phys. Rev. Lett. 70, 2802 (1993).
- [5] E. Vescovo, C. Carbone, W. Eberhardt, O. Rader, T. Kachel, and W. Gudat, Spin-resolved photoemission study of the clean and oxygen-covered Fe(110) surface, Phys. Rev. B 48, 285 (1993).
- [6] H.-J. Kim., E. Vescovo, S. Heinze, and S. Blügel, Surface electronic structure of Fe(110): the importance of surface resonances, Surf. Sci. 478, 193 (2001).
- [7] J. Braun, C. Math, A. Postnikov, and M. Donath, Surface resonances versus surface states on Fe(110), Phys. Rev. B 65, 184412 (2002).
- [8] J. Schäfer, D. Schrupp, E. Rotenberg, K. Rossnagel, H. Koh, P. Blaha, and R. Claessen, Electronic quasiparticle renormalization on the spin wave energy scale, Phys. Rev. Lett. 92, 097205 (2004).
- [9] J. Schäfer, M. Hoinkis, D. Schrupp, E. Rotenberg, P. Blaha, and R. Claessen, Electronic Quasiparticles and evolution of Fermi level spin states in thin magnetic layers, Surf. Sci. 600, 3912 (2006).
- [10] J. Sánchez-Barriga, J. Fink, V. Boni, I. Di Marco, J. Braun, J. Minár, A. Varykhalov, O. Rader, V. Bellini, F. Manghi, H. Ebert, M. I. Katsnelson, A. I. Lichtenstein, O. Eriksson, W. Eberhardt, and H. A. Dürr, Strength of correlation effects in the electronic structure of iron, Phys.

- Rev. Lett. **103**, 267203 (2009).
- [11] Y.-J. Chen, J.-P. Hanke, M. Hoffmann, G. Bihlmayer, Y. Mokrousov, S. Blügel, C. M. Schneider, and C. Tusche, Spanning Fermi arcs in a two-dimensional magnet, Nat. Comm 13, 5309 (2022).
- [12] D. Gosálbez-Martínez, I. Souza, and D. Vanderbilt, Chiral degeneracies and Fermi-surface Chern numbers in bcc Fe, Phys. Rev. B **92**, 1 (2015).
- [13] D. Gosálbez-Martínez, G. Autès, and O. V. Yazyev, Topological Fermi-arc surface resonances in bcc iron, Phys. Rev. B **102**, 035419 (2020).
- [14] W. H. Butler, X.-G. Zhang, T. C. Schulthess, and J. M. MacLaren, Spin-dependent tunneling conductance of Fe|MgO|Fe sandwiches, Phys. Rev. B 63, 054416 (2001).
- [15] A. N. Chantis, K. D. Belashchenko, E. Y. Tsymbal, and I. V. Sus, The importance of Fe surface states for magnetic tunnel junction based spintronic devices, Modern Physics Letters B 22, 2529 (2008).
- [16] L. Plucinski, Y. Zhao, C. M. Schneider, B. Sinkovic, and E. Vescovo, Surface electronic structure of ferromagnetic Fe(001), Phys. Rev. B 80, 184430 (2009).
- [17] A. N. Chantis, K. D. Belashchenko, E. Y. Tsymbal, and M. van Schilfgaarde, Tunneling anisotropic magnetoresistance driven by resonant surface states: First-principles calculations on an Fe(001) surface, Phys. Rev. Lett. 98, 046601 (2007).
- [18] K. Nakamura, R. Shimabukuro, T. Akiyama, T. Ito, and A. J. Freeman, Origin of electric-field-induced modification of magnetocrystalline anisotropy at Fe(001) surfaces: Mechanism of dipole formation from first principles, Phys. Rev. B 80, 172402 (2009).
- [19] M. Escher, N. B. Weber, M. Merkel, L. Plucinski, and C. M. Schneider, Ferrum: A new highly efficient spin detector for electron spectroscopy, e-Journal of Surface Science and Nanotechnology 9, 340 (2011).
- [20] E. Vescovo, O. Rader, and C. Carbone, Spin-polarized surface states of Fe(100), Phys. Rev. B 47, 13051 (1993).
- [21] P. Johnson, Y. Cchang, N. B. Brookes, and M. Weinert, Potassium adsorption and an unoccupied surface state on fe(001), J. Phys. Cond.Matter 10, 95 (1998).
- [22] C. Eibl, A. Schmidt, and M. Donath, Appearance of the minority  $d_{z^2}$  surface state and disappearance of the image-potential state: Criteria for clean Fe(001), Phys. Rev. B **86**, 161414 (2012).

- [23] A. M. Turner and J. L. Erskine, Surface electronic properties of Fe(100), Phys. Rev. B 30, 6675 (1984).
- [24] E. Młyńczak, M. Eschbach, S. Borek, J. Minár, J. Braun, I. Aguilera, G. Bihlmayer, S. Döring, M. Gehlmann, P. Gospodarič, S. Suga, L. Plucinski, S. Blügel, H. Ebert, and C. M. Schneider, Fermi surface manipulation by external magnetic field demonstrated for a prototypical ferromagnet, Phys. Rev. X 6, 041048 (2016).
- [25] E. Młyńczak, M. C. T. D. Müller, P. Gospodarič, T. Heider, I. Aguilera, M. Gehlmann, M. Jugovac, G. Zamborlini, C. Tusche, S. Suga, V. Feyer, L. Plucinski, C. Friedrich, S. Blügel, and C. M. Schneider, Kink far below the Fermi level reveals new electron-magnon scattering channel in Fe, Nat. Comm. 10, 505 (2019).
- [26] E. Młyńczak, I. Aguilera, P. Gospodarič, T. Heider, M. Jugovac, G. Zamborlini, C. Tusche, S. Suga, V. Feyer, S. Blügel, L. Plucinski, and C. M. Schneider, Spin-polarized quantized electronic structure of Fe(001) with symmetry breaking due to the magnetization direction, Phys. Rev. B 103, 035134 (2021).
- [27] E. Młyńczak, I. Aguilera, P. Gospodarič, T. Heider, M. Jugovac, G. Zamborlini, J.-P. Hanke, C. Friedrich, Y. Mokrousov, C. Tusche, S. Suga, V. Feyer, S. Blügel, L. Plucinski, and C. M. Schneider, Fe(001) angle-resolved photoemission and intrinsic anomalous hall conductivity in Fe seen by different ab initio approaches: LDA and GGA versus GW, Phys. Rev. B 105, 115135 (2022).
- [28] A. N. Chantis, D. L. Smith, J. Fransson, and A. V. Balatsky, Scanning tunneling microscopy detection of spin polarized resonant surface bands: The example of Fe(001), Phys. Rev. B 79, 165423 (2009).
- [29] M. Szczepanik-Ciba, T. Sobol, and J. Szade, Phelix a new soft x-ray spectroscopy beamline at solaris synchrotron, Nucl. Instrum. Methods Phys. Res. B **492**, 49 (2021).
- [30] R. Hammer, A. Sander, S. Förster, M. Kiel, K. Meinel, and W. Widdra, Surface reconstruction of au(001): High-resolution real-space and reciprocal-space inspection, Phys. Rev. B 90, 035446 (2014).
- [31] E. Moog and S. Bader, Smoke signals from ferromagnetic monolayers: p(1×1) Fe/Au(100), Superlattices and Microstructures 1, 543 (1985).
- [32] W. Dürr, M. Taborelli, O. Paul, R. Germar, W. Gudat, D. Pescia, and M. Landolt, Magnetic Phase Transition in Two-Dimensional Ultrathin Fe Films on Au(100), Phys. Rev. Lett. 62,

- 206 (1989).
- [33] http://www.flapw.de.
- [34] V. Strocov, Intrinsic accuracy in 3-dimensional photoemission band mapping, Journal of Electron Spectroscopy and Related Phenomena 130, 65 (2003).
- [35] R. Matzdorf, Uv-photoelectron spectroscopy at highest resolution —direct access to lifetime effects in solids?, Applied Physics A 63, 549 (1996).
- [36] C. S. Wang and A. J. Freeman, Surface states, surface magnetization, and electron spin polarization: Fe(001), Phys. Rev. B 24, 4364 (1981).
- [37] M. C. T. D. Müller, S. Blügel, and C. Friedrich, Electron-magnon scattering in elementary ferromagnets from first principles: Lifetime broadening and band anomalies, Phys. Rev. B 100, 045130 (2019).
- [38] C. H. Chang, K. P. Dou, G. Y. Guo, and C. C. Kaun, Quantum-well-induced engineering of magnetocrystalline anisotropy in ferromagnetic films, NPG Asia Materials 9, e424 (2017).
- [39] D. M. Janas, A. Droghetti, S. Ponzoni, I. Cojocariu, M. Jugovac, V. Feyer, M. M. Radonjić, I. Rungger, L. Chioncel, G. Zamborlini, and M. Cinchetti, Enhancing electron correlation at a 3d ferromagnetic surface, Advanced Materials 35, 2205698 (2023).
- [40] G. Bihlmayer, P. Noël, D. V. Vyalikh, E. V. Chulkov, and A. Manchon, Rashba-like physics in condensed matter, Nat. Rev. Phys. 4, 642 (2022).
- [41] S. E. Barnes, J. Ieda, and S. Maekawa, Rashba spin-orbit anisotropy and the electric field control of magnetism, Sci. Rep 4, 4105 (2014).
- [42] O. Krupin, G. Bihlmayer, K. M. Döbrich, J. E. Prieto, K. Starke, S. Gorovikov, S. Blügel, S. Kevan, and G. Kaindl, Rashba effect at the surfaces of rare-earth metals and their monoxides, New Journal of Physics 11, 013035 (2009).
- [43] O. Krupin, G. Bihlmayer, K. Starke, S. Gorovikov, J. E. Prieto, K. Döbrich, S. Blügel, and G. Kaindl, Rashba effect at magnetic metal surfaces, Phys. Rev. B 71, 201403 (2005).
- [44] P. Moras, G. Bihlmayer, P. M. Sheverdyaeva, S. K. Mahatha, M. Papagno, J. Sánchez-Barriga, O. Rader, L. Novinec, S. Gardonio, and C. Carbone, Magnetization-dependent rashba splitting of quantum well states at the Co/W interface, Phys. Rev. B 91, 195410 (2015).
- [45] P. Hofmann, C. Søndergaard, S. Agergaard, S. V. Hoffmann, J. E. Gayone, G. Zampieri, S. Lizzit, and A. Baraldi, Unexpected surface sensitivity at high energies in angle-resolved photoemission, Phys. Rev. B 66, 245422 (2002).

[46] Z. Liu, Y. L. Chen, J. G. Analytis, S. K. Mo, D. H. Lu, R. G. Moore, I. R. Fisher, Z. Hussain, and Z. X. Shen, Robust topological surface state against direct surface contamination, Physica E 44, 891 (2012).